Research Square

Preprints are preliminary reports that have not undergone peer review.
They should not be considered conclusive, used to inform clinical practice,
or referenced by the media as validated information.

# Oeosporangium elegans Adapts to Desiccated State Upon Reprogramming Metabolism Through Redox Balance, Membrane Dynamics, and Protective Mechanisms

**Hosahalli Somasundara Reddy Rudresh**
Tumkur University
**Hulikall Shivashankara Santhosh Kumar**
Kuvempu University
**Manjunath B Joshi**
Manipal Academy of Higher Education
**Srinivas Mutalik**
Manipal Academy of Higher Education
**Ramasandra Govind Sharathchandra**
Tumkur University
**Vasudev Pai**
pai.vasudev@manipal.edu

Manipal Academy of Higher Education

**Article**

**Keywords:** Desiccation, Metabolites, LC MS/MS, Stress response Pathways, Pheophorbide a

**Posted Date:** August 14th, 2026

**DOI:** https://doi.org/10.21203/rs.3.rs-10510745/v1

**License:** This work is licensed under a Creative Commons Attribution 4.0 International License.
Read Full License

**Additional Declarations:** No competing interests reported.

# *Oeosporangium elegans* Adapts to Desiccated State Upon Reprogramming Metabolism Through Redox Balance, Membrane Dynamics, and Protective Mechanisms

Hosahalli Somasundara Reddy Rudresh [a], Hulikall Shivashankara Santhosh Kumar [b], Manjunath B Joshi [c], Srinivas Mutalik [d], Ramasandra Govind Sharathchandra [a*], Vasudev Pai [d*].

[a] Department of Studies and Research in Microbiology, Tumkur University, Tumkur, Karnataka, India-572102

[b] Department of Studies and Research in Biotechnology and Bioinformatics, Kuvempu University, Shimogga, Karnataka, India-577515

[c] Department of Ageing Research, Manipal Academy of Higher Education, Manipal, India - 576104

[d] Department of Pharmacognosy, Manipal College of Pharmaceutical Sciences, Manipal Academy of Higher Education, Manipal, India - 576104

**Author for correspondence**: **1. Dr. Vasudev Pai**

Department of Pharmacognosy, Manipal College of Pharmaceutical Sciences,

Manipal Academy of Higher Education, Manipal, India - 576104

pai.vasudev@manipal.edu

ORCID ID – 0000 0002 5147 6389

**Co-Correspondence:** **2. Dr. Ramasandra Govind Sharathchandra**

Professor and Chairman

Department of Studies and Research in Microbiology, Tumkur University

rgschandra@gmail.com

ORCID ID – 0000 0002 1156 9986

**Abstract:**

Desiccation tolerance (DT) in plants involves complex metabolic reprogramming that enables survival under severe water deficit conditions. In this study, a comparative metabolomic analysis was conducted to investigate metabolic shift between hydrated and desiccated states of *Oeosporangium elegans*. A total of 798 metabolites were identified, out of which 268 (33.6%) were unique to the hydrated state, 298 (37.3%) were specific to the desiccated state, and 232 (29.1%) were common to both conditions with differential abundance. Pathway enrichment analysis revealed that metabolites of the hydrated stage participate in biosynthetic and growth-associated pathways, including carbohydrate metabolism, nucleotide biosynthesis, and flavonoid biosynthesis. In the desiccated stage, the profile shifted toward stress-responsive metabolism, with enrichment of riboflavin metabolism, pyrimidine metabolism, and biosynthesis of unsaturated fatty acids. Pathways supporting redox homeostasis, membrane stabilization, and molecular repair under water deficit accompanied this shift. Although metabolite detected only in the desiccated stage, pheophorbide a, an intermediate of chlorophyll degradation, is proposed as a candidate biomarker of desiccation stress. Considering both stages together, the findings indicate that DT in *Oeosporangium elegans* depends on coordinated metabolic networks spanning redox balance, membrane dynamics, and protective mechanisms.

**Key Words:** *Desiccation, Metabolites, LC MS/MS, Stress response Pathways, Pheophorbide a.*

## 1. Introduction:

Desiccation represents one of the most extreme abiotic stresses encountered by plants. Characterized by the loss of more than 70% of cellular water content, this condition disrupts cellular homeostasis. In most species, such severe water deficit produces irreversible damage, including membrane disintegration, protein denaturation, and oxidative damage arising from redox imbalance. This breakdown of homeostasis can ultimately cause cell death in sensitive plants. Although the majority of species fail to survive water loss of this magnitude, a small group known as desiccation tolerant (DT) plants withstands desiccation and resumes normal metabolic function upon rehydration. These plants exhibit a phenomenon called anhydrobiosis - "life without water." This ability reflects a highly regulated transition from active metabolism to a desiccated state and vice versa with stabilized cellular structures (Oliver et al., 2020; Alejo-Jacuinde & Herrera-Estrella, 2022; Li et al., 2023).

Water loss in DT plants triggers extensive metabolic reprogramming that sustains cellular function even as tissue moisture falls to severe levels. Several protective mechanisms operate at once, and survival rests on this integrated physiological and biochemical response (Oliver et al., 2020). Among the compounds that accumulate, soluble carbohydrates, secondary metabolites, lipid-derived compounds, and antioxidants constitute the core of the response. Working across multiple cellular targets, these metabolites stabilize proteins and membranes, hold cellular architecture intact through dehydration, and limit oxidative damage caused by stress induced reactive oxygen species (ROS) (Challabathula & Bartels, 2013; Farrant et al., 2015; Oliver et al., 2020).

Throughout cellular dehydration, protective processes depend largely on the metabolites that mediate the DT response. Soluble sugars and related osmolytes maintain osmotic balance, reduce the structural consequences of water loss, and preserve cellular organization. Because they scavenge free radicals efficiently, flavonoids and other phenolic compounds limit accumulation of ROS and shield proteins, lipids, and nucleic acids from oxidative damage. Lipid-derived metabolites contribute to membrane stability by sustaining fluidity and guarding against structural disruption. Beyond direct protection, several secondary metabolites function in stress perception and signalling, coordinating the protective mechanisms that follow. Collectively, these metabolite groups form an integrated biochemical network that strengthens cellular resilience and supports survival under desiccation stress (Krasensky & Jonak, 2012; Challabathula & Bartels, 2013; Bentley et al., 2019).

Comprehensive profiling of metabolites that respond to cellular dehydration allows metabolomics to address DT at a systems level. Metabolites shared between hydrated and desiccated states, when compared with those uniquely accumulated during desiccation, distinguish constitutive metabolism from adjustments triggered by water deficit. Integration of these profiles with pathway enrichment analysis further reveals coordinated biochemical reprogramming and identifies the metabolic pathways that underpin DT (Challabathula & Bartels, 2013; Dace et al., 2023).

Characterizing desiccation-associated metabolic pathways also has broader implications for crop improvement. Metabolic pathways preferentially activated during desiccation may represent targets for genetic and metabolic engineering aimed at enhancing drought resilience by reinforcing antioxidant capacity, maintaining membrane integrity, and improving metabolic adaptation to water limitation. Consequently, identifying conserved metabolic signatures of DT may provide a foundation for developing stress-resilient crops (Dace et al., 2023; Liu et al., 2023).

In the present study, we analyse the metabolomic profile of the DT fern *Oeosporangium elegans*. As a monilophyte, *O. elegans* occupies an intermediate evolutionary position among vascular plants, sharing a closer evolutionary relationship with seed plants than with lycophytes such as *Selaginella*. *O. elegans* can lose more than 90% (198 hours) of its relative water content and regain up to 95% (12 hours) under rehydration conditions (Rudresh et al., 2023).

## 2. Results and Discussion:

A comparative analysis of metabolite profile between hydrated and desiccated states revealed stage specific metabolites. A total of 268 metabolites (33.6%) were uniquely detected in the hydrated state, while 298 metabolites (37.3%) were in the desiccated condition. In addition, 232 metabolites (29.1%) were common to both states with different levels of expression.

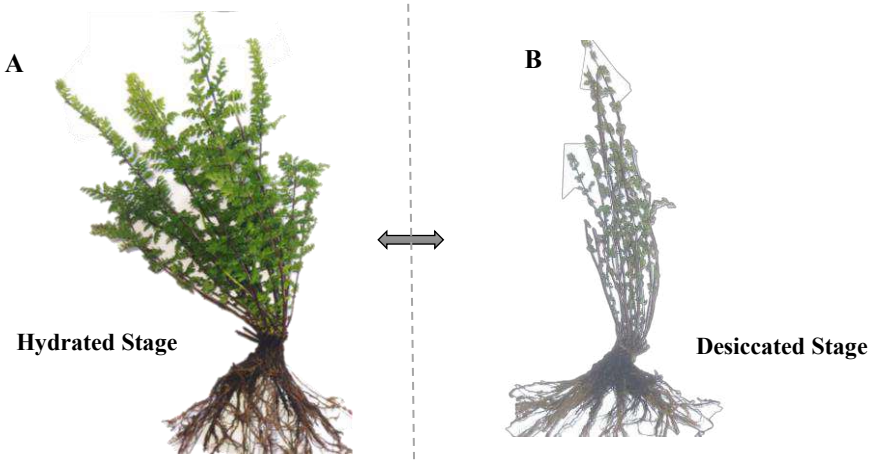



**Figure 01: Morphology of *Oeosporangium elegans* in hydrated (A) and desiccated stage (B).**

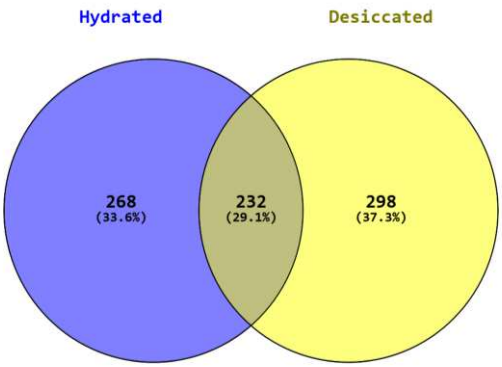



**Figure 02. Venn diagram illustrating the distribution of metabolites identified in hydrated and desiccated states. The figure was constructed using the *Venny 2.1.0*, online tool (Oliveros, J.C. 2015).**

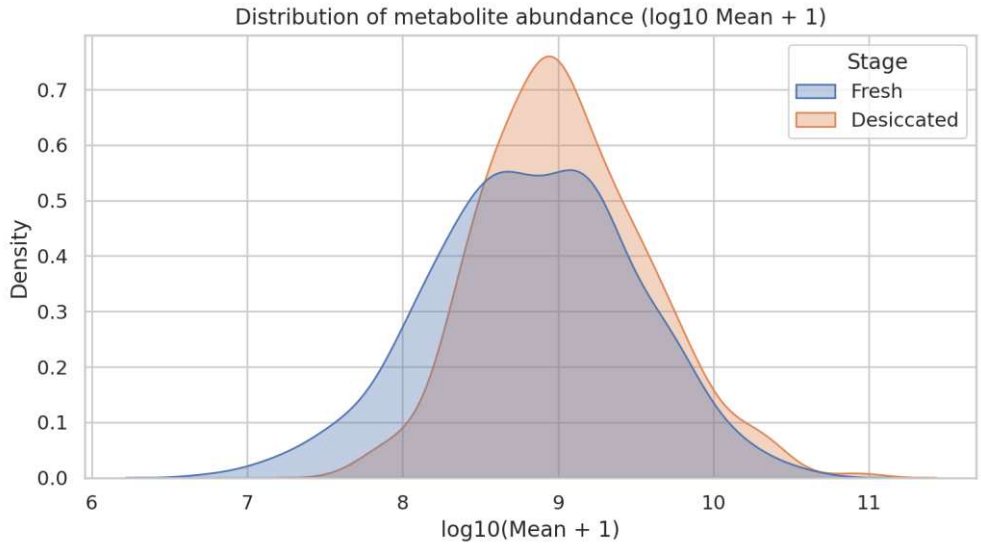



**Figure 03. Kernel density plot illustrating the distribution of metabolite abundance in hydrated and desiccated samples following log10 transformation of mean values [log10(mean + 1)].**

The kernel density plot showed that, the hydrated samples show a broader distribution of metabolites, whereas the desiccated samples exhibit a relatively shifted profile, reflecting alterations in metabolite accumulation under desiccation. The overlap between the two distribution indicates shared metabolites across conditions. More number of unique metabolites detected in desiccated samples indicates a pronounced metabolic reprogramming in response to water deficit.

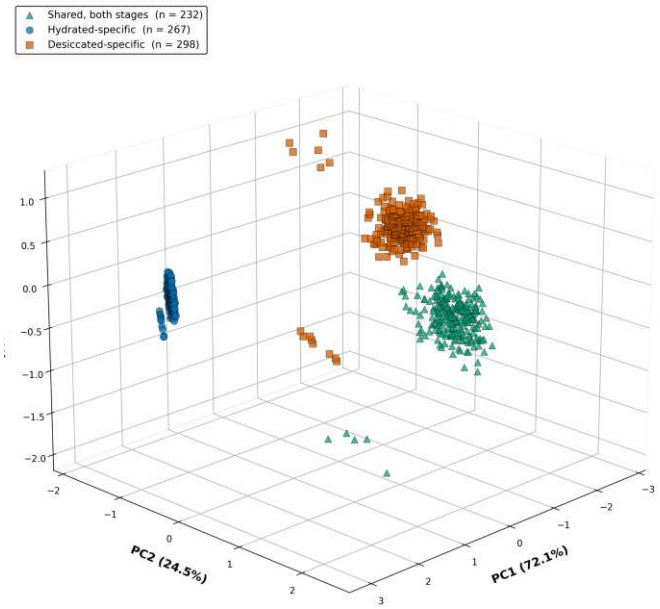



**Figure 04. Three-dimensional principal component analysis (3D-PCA) of the complete metabolome of *Oeosporangium elegans*.**

Three-dimensional principal component analysis (3D-PCA) of 797 metabolites resolved three clusters: hydrated-specific (n = 267), desiccated-specific (n = 298), and shared (n = 232). The first three components accounted for 97.8% of the total variance. PC1 explained 72.1% and PC2 a further 24.5%, so two dimensions were sufficient to describe nearly all metabolic variation. Hydrated-specific metabolites separated along PC1, whereas PC2 resolved the desiccated-specific group from the shared metabolites. Overlap between clusters was minimal, which indicates that the three categories differ in metabolite composition. Metabolites grouped tightly within each cluster, and the few outliers were compounds with unique accumulation patterns. The ordination therefore shows clear metabolic differentiation between the hydrated and desiccated states of *Oeosporangium elegans*.

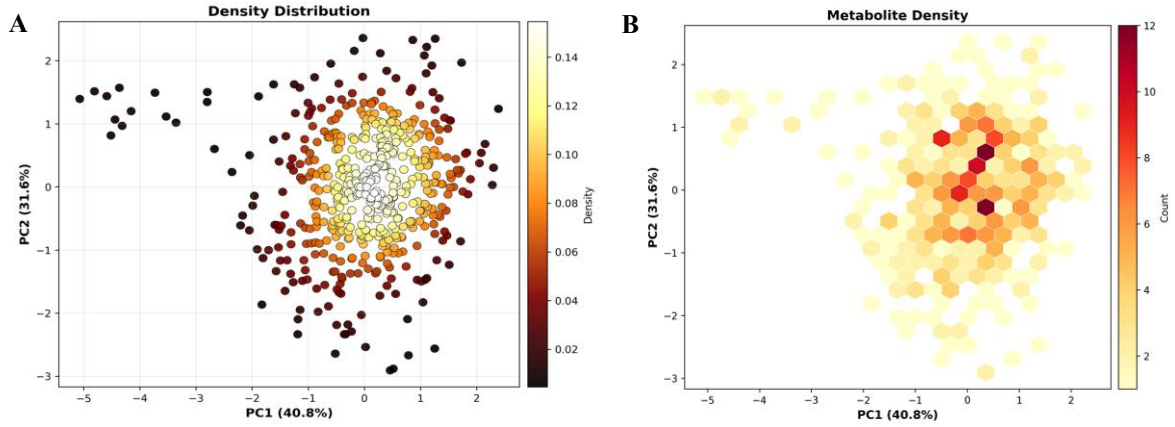



**Figure 05. Distribution of 530 hydrated-associated metabolites. (A) Kernel density scatter plot of metabolites projected onto PC1 (40.8%) and PC2 (31.6%). (B) Hexagonal density map showing metabolite frequency within the same PCA space.**

Distribution analysis of the 530 hydrated-associated metabolites showed a compact arrangement within the PC1–PC2 ordination space. PC1 accounted for 40.8% of the total variance and PC2 for 31.6%. Kernel density and hexagonal density analyses each identified a central high-density cluster that contained most of the metabolites, with only a few at the periphery. Spread beyond this cluster was limited, and the low dispersion across the ordination space confirms that hydrated-associated metabolites occupy a narrow region.

Comparison of the two stages showed differences in metabolite organization within the PC1–PC2 space. Hydrated-stage metabolites formed a compact, high-density cluster. Desiccated-stage metabolites spread more widely, and a greater proportion of them extended toward the periphery. A well-defined central core was present in both stages, but the wider spread under desiccation points to greater variability in metabolite distribution during dehydration. The density analyses are descriptive and do not test for statistical differences between the stages. Their distribution patterns match the PCA and metabolite-profiling results, which show that desiccation coincides with a reorganization of the metabolome relative to the hydrated state.

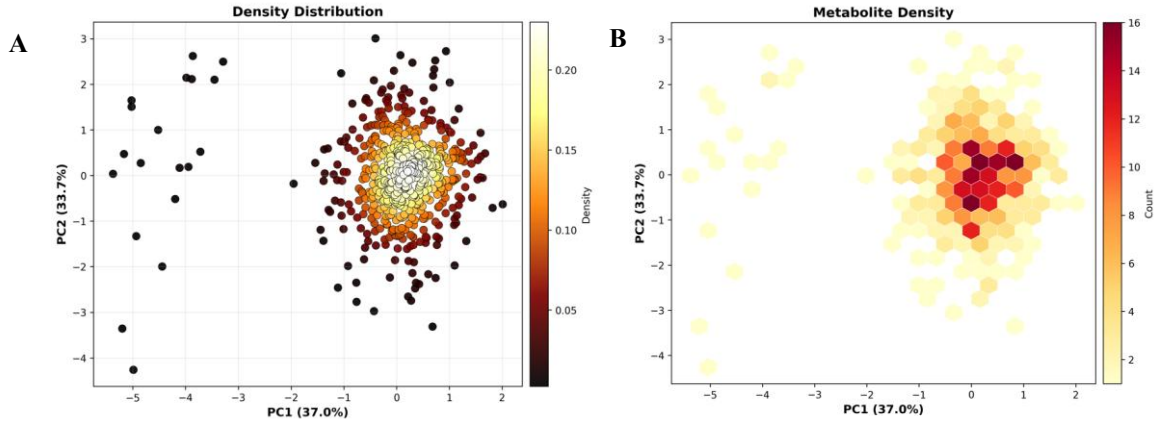



**Figure 06. Distribution analysis of desiccation-associated metabolites. (A) Kernel density scatter plot of 530 desiccation-associated metabolites projected onto PC1 (37.0%) and PC2 (33.7%). (B) Hexagonal density map showing metabolite frequency within the same PCA space, with colour intensity indicating increasing metabolite density.**

Distribution analysis of the 530 desiccation-associated metabolites showed that most metabolites formed a compact, high-density cluster within the PC1–PC2 space, with only a few metabolites occurring as dispersed outliers. The kernel density and hexagonal density plots consistently identified a central region containing the greatest metabolite concentration, indicating that the desiccated metabolome is characterized by a dominant group of metabolites with similar multivariate patterns. The relatively small number of peripheral metabolites suggests the presence of metabolites with distinct abundance profiles during desiccation. This structured distribution supports coordinated metabolic reorganization under dehydration and complements the PCA results by demonstrating that the desiccation-associated metabolome is organized around a well-defined metabolic core rather than exhibiting random variability.

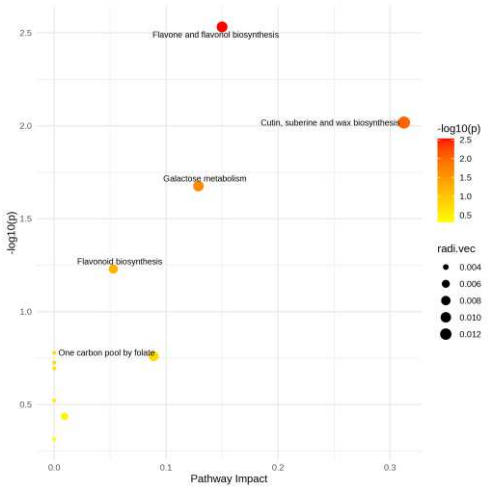



**Figure 07. Pathway enrichment analysis of metabolites in the hydrated state. Bubble plot representing metabolic pathway analysis of metabolites identified under hydrated conditions, generated using MetaboAnalyst.**

**2.1 Metabolic Pathways in the Hydrated State:**

Pathway enrichment analysis of hydrated-stage metabolites identified pathways associated mainly with primary metabolism, cellular maintenance, and constitutive protective processes. Flavone and flavonol biosynthesis, together with the broader flavonoid biosynthesis pathway, ranked among the most significantly enriched. Enrichment of these pathways indicates flavonoid-associated metabolism under hydrated conditions, which is consistent with constitutive production of secondary metabolites that contribute to cellular protection and physiological regulation.

Carbohydrate metabolism was well represented, and both galactose metabolism and starch and sucrose metabolism were significantly enriched. Enrichment of these pathways indicates active carbohydrate turnover and a steady supply of intermediates for energy metabolism and biosynthesis in the hydrated state. Folate and pyrimidine metabolism showed comparable enrichment, which reflects active nucleotide-associated metabolism, since both pathways connect to one-carbon metabolism and nucleotide biosynthesis. α-Linolenic acid metabolism was enriched alongside cutin, suberin, and wax biosynthesis, indicating continued lipid turnover and synthesis of protective barriers under hydrated conditions. Amino sugar and nucleotide sugar metabolism was also enriched. This pathway supplies structural carbohydrate precursors and glycosylated metabolites required for cell wall metabolism. Considered together, these results define the hydrated metabolome through enrichment of flavonoid biosynthesis, carbohydrate metabolism, nucleotide metabolism, lipid metabolism, and structural carbohydrate biosynthesis. This coordinated pattern shows that hydrated tissues sustain a metabolically active state built on primary metabolism together with constitutive protective metabolism.

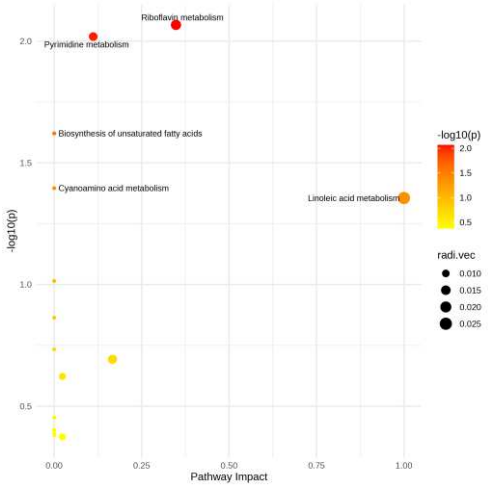



**Figure 08. Pathway enrichment analysis of metabolites in the desiccated state. (A) Bubble plot illustrating the results of pathway enrichment analysis of metabolites identified under desiccated conditions, generated using MetaboAnalyst (version 5.0).**

**2.2 Metabolic Pathways Predominant in the Desiccated State:**

Enrichment analysis of the desiccated metabolome showed a shift in cellular metabolism away from the hydrated profile. Riboflavin metabolism ranked as the most significantly enriched pathway, a result that points to heightened flavin-associated metabolism during desiccation. The pathway supplies the flavin cofactors FAD and FMN, both central to cellular redox reactions. Its enrichment occurred alongside antioxidant-related metabolism,

which suggests greater metabolic investment in redox balance under severe dehydration. Flavin-dependent metabolism thus forms a defining feature of the desiccated profile of *Oeosporangium elegans*.

Pyrimidine metabolism was also significantly enriched in the desiccated state and reflects active nucleotide-associated metabolism under dehydration. Sustained nucleotide turnover and cellular maintenance through desiccation agree with this observation (Moffatt & Ashihara, 2002; Stasolla et al., 2003).

Three lipid pathways were enriched: unsaturated fatty acid biosynthesis, linoleic acid metabolism, and arachidonic acid metabolism. Their joint enrichment indicates a substantial reorganization of lipid metabolism during dehydration. Each pathway acts on distinct substrates, but all three govern membrane lipid remodelling and preserve membrane function under water deficit, in line with their established roles in DT (He & Ding, 2020).

The enrichment of nicotinate and nicotinamide metabolism, along with lipoic acid metabolism, further highlights the importance of redox regulation under desiccation. These pathways are involved in maintaining cellular pools of $NAD^+$ and $NADP^+$, as well as other essential cofactors required for antioxidant enzyme activities. Their increased activity suggests a heightened demand for efficient energy management and detoxification mechanisms to sustain cellular function under stress conditions (Berglund & Ohlsson, 2025).

In addition, cutin, suberin, and wax biosynthesis pathways indicate structural adaptations that minimize water loss. These compounds form protective barriers that reduce permeability and enhance resistance to desiccation. Such structural modifications complement intracellular metabolic adjustments, contributing to overall stress resilience ( Schuster et al., 2016; Harman-Ware et al., 2021; Suresh et al., 2022).

The enrichment of cyanoamino acid metabolism and amino acid related pathways, such as cysteine and methionine metabolism and lysine degradation, suggests a role in detoxification and osmotic regulation. These pathways may facilitate the removal of toxic intermediates and support the synthesis of stress-related metabolites, including antioxidants and compatible solutes (Heidarzadeh, 2025).

Although detected with relatively lower significance, flavonoid biosynthesis also contributes to DT through its role in antioxidant defense. Flavonoids are known to scavenge ROS and protect against oxidative stress, thereby supporting cellular survival during water stress (Dace et al., 2023).

Hydrated samples were dominated by biosynthetic and growth-related pathways, whereas desiccated samples exhibited protective, repair, and stabilization mechanisms. Taken together, these results reflect adaptive metabolic reprogramming in response to desiccation stress.

### 2.3 Metabolites Ranked by Mean Abundance

Metabolites were ranked according to their mean abundance using RDKit-based analysis, and the ten most abundant metabolites from the hydrated and desiccated stages were selected. Four metabolites from the hydrated stage and three from the desiccated stage were identified as probable plastic contaminants or non-biological artefacts and were excluded from further analyses. Subsequent interpretation was therefore restricted to biologically relevant metabolites.

#### 2.3.1 Metabolites in Hydrated Stage based on Mean Abundance

| Sl. No. | Metabolite | Mean Abundance | HMDB ID |
|---|---|---|---|
| 1. | (2Z)-3-[4,5-Dihydroxy-2-(2-hydroxy-2-propanyl)-2,3-dihydro-1-benzofuran-7-yl]acrylic acid | $3.53 \times 10^{10}$ | -- |
| 2. | Ala-Hyp-Gly | $3.16 \times 10^{10}$ | |
| 3. | Esculin | $2.17 \times 10^{10}$ | HMDB0030820 |
| 4. | Aspartylphenylalanine | $1.80 \times 10^{10}$ | HMDB0000706 |
| 5. | Prunin | $1.74 \times 10^{10}$ | -- |
| 6. | Genkwanin | $1.46 \times 10^{10}$ | HMDB0252684 |

**Table 01. List of predominant metabolites detected in the hydrated samples along with their corresponding mean abundance values. Mean abundance values represent the average intensity of each metabolite across hydrated stage.**

Phenolic compounds such as (2Z)-benzofuran acrylic acid derivative, esculin, prunin, and genkwanin indicate an active phenylpropanoid pathway, which plays a central role in maintaining redox balance and protecting cells from routine oxidative stress. These metabolites function as antioxidants and UV-protective compounds, supporting cellular integrity during normal metabolic activity. Their glycosylated or methylated forms suggest stable storage and controlled utilization under non-stress conditions (Ramaroson et al., 2022; Singh et al., 2023).

The presence of peptide metabolites such as Ala-Hyp-Gly and aspartylphenylalanine reflects active protein turnover and cell wall remodelling. Hydroxyproline-containing peptides are associated with extensin dynamics, which are essential for cell wall expansion and structural flexibility during growth. This indicates that hydrated tissues maintain a dynamic balance between synthesis and degradation of structural proteins ( Lamport et al., 2011; Ivakov et al., 2017).

**2.3.2 Metabolites in Desiccated Stage based on Mean Abundance**

| Sl. No. | Metabolite | Mean Abundance | HMDB ID |
|---|---|---|---|
| 1. | Arachidoyl Ethanolamide | $2.53 \times 10^{10}$ | HMDB0013655 |
| 2. | 4-methoxy-7-glycosyloxymethyl furochromone | $2.50 \times 10^{10}$ | -- |
| 3. | Yuccagenin | $2.31 \times 10^{10}$ | -- |
| 4. | Caffeoyl tyrosine | $1.96 \times 10^{10}$ | HMDB0029295 |
| 5. | Pheophorbide a | $1.64 \times 10^{10}$ | METPA1634 |
| 6. | Epicatechin | $1.57 \times 10^{10}$ | HMDB0001871 |
| 7. | 3-hydroxypentadecanoic acid | $1.54 \times 10^{10}$ | HMDB0061657 |

**Table 02. List of predominant metabolites detected in the desiccated stage along with their corresponding mean abundance values. The metabolites were processed using RD-Kit-based analysis. Mean abundance values represent the average intensity of each metabolite across desiccated stage.**

#### 2.3.1.1 Arachidoyl Ethanolamide ($C_{22}H_{45}NO_2$): Synonyms: Eicosanoyl-EA, N-eicosanoyl-ethanolamine, Ref. Chem:1084061, and N-(2-hydroxyethyl)icosanamid (PubChem, 2026.).

Arachidoyl ethanolamide (N-arachidoyl ethanolamine; C20:0-EA), a member of the N-acylethanolamine (NAE) family, was detected in the desiccated stage of *Oeosporangium elegans*, indicating that NAE metabolism forms part of the lipid remodelling associated with desiccation. NAEs are generated from N-acyl phosphatidylethanolamines (NAPEs), and their composition generally reflects the fatty acid profile of membrane lipids. Thus, the occurrence of arachidoyl ethanolamide is consistent with stress-induced membrane turnover and the reorganization of lipid metabolism during dehydration (Blancaflor et al., 2014). Although NAEs have been implicated in plant development and responses to environmental stress, arachidoyl ethanolamide has received little attention in plant systems, making its detection in *O. elegans*.

Previous studies have shown that NAEs participate in developmental regulation and stress adaptation, particularly during seed desiccation and germination, where elevated NAE levels are associated with growth arrest and maintenance of the desiccated state (Chapman et al., 1998; Chapman, 2004; Blancaflor et al., 2014). NAEs have also been reported to interact with abscisic acid (ABA)-mediated signalling, suggesting a broader role in coordinating stress responses (Teaster et al., 2007; Blancaflor et al., 2014). Whether arachidoyl ethanolamide performs similar regulatory functions in *O. elegans*.

To our knowledge, arachidoyl ethanolamide has not previously been reported in association with DT in plants. Its occurrence in desiccated *O. elegans* therefore expands the range of NAEs implicated in dehydration responses and identifies this saturated lipid as a candidate metabolite for future functional studies.

#### 2.3.1.2 4-methoxy-7-glycosyloxymethyl furochromone

4-Methoxy-7-glycosyloxymethyl furochromone, a phenolic secondary metabolite is structurally similar to chromone and flavonoid compounds. It is likely associated with phenylpropanoid-derived metabolism. Phenolic compounds are well recognized for their roles in plant stress responses. They act as antioxidants and photoprotective molecule. The accumulation of such metabolites suggests activation of secondary metabolic pathways involved in ROS scavenging and protection against photooxidative damage under desiccation (Agati & Tattini, 2010; Vogt, 2010; Brunetti et al., 2013).

The identification of 4-methoxy-7-glycosyloxymethyl furochromone in this study represents a previously unreported metabolite in the context of DT, suggesting a potential but unexplored role of furochromone derivatives in stress adaptation.

#### 2.3.1.3 Yuccagenin

Yuccagenin is a steroidal sapogenin derived from the terpenoid backbone biosynthesis pathway, representing an important class of secondary metabolites associated with plant adaptation to extreme dehydration stress. Water loss imposes severe biophysical constraints on cellular membranes, including disruption of hydration shells, increased lipid packing, and phase transitions that can compromise membrane integrity. Under such conditions, maintaining membrane stability becomes essential for cellular survival (Upchurch, 2008; Shajar et al., 2025; Dong & Qi, 2025).

Yuccagenin also acts as steroidal saponin precursor, which is implicated in stress-responsive metabolic modifications. The accumulation of yuccagenin suggests activation of terpenoid metabolism. Which is associated with protective responses under abiotic stress. These metabolites may also participate in regulating stress signalling pathways and cellular homeostasis during desiccation ( Osbourn, 1996; Isah, 2019).

Furthermore, desiccation is often accompanied by oxidative stress due to impaired electron transport and increased production of ROS. Yuccagenin may limit the lipid peroxidation by free radicals and reduce ROS propagation within cellular compartments by stabilizing membrane structures. This indirect protective role complements the action of phenolic antioxidants to indicating coordinated interaction between lipid-derived and phenolic defense systems (Upchurch, 2008; Isah, 2019).

Although yuccagenin is known as a steroidal sapogenin involved in plant defense and membrane interactions. Its role in DT has not been documented. Its detection in the present study is a potentially novel observation. Its accumulation highlights the importance of steroidal components in preserving cellular integrity during desiccation. It also demonstrates that DT in *Oeosporangium elegans* is driven by integrated metabolic reprogramming involving both lipid stabilization and antioxidant defense mechanisms.

#### 2.3.1.4 Caffeoyl tyrosine

Caffeoyl tyrosine is a conjugated phenolic metabolite formed from caffeic acid and tyrosine, and it acts as an intermediate of the phenylpropanoid pathway. Phenolic conjugates of this class form part of plant secondary metabolism under abiotic stress. Desiccation imposes severe oxidative stress by disrupting cellular homeostasis and increasing ROS generation (Farrant, 2000; Michalak, 2006). Phenolic conjugates also support photoprotection, since they filter excess ultraviolet radiation and limit photooxidative damage under high light. Such protection is relevant in exposed habitats, where desiccation coincides with intense solar irradiance. A second function of phenylpropanoid-derived metabolites is structural: they reinforce the cell wall through lignin and related components, which strengthens mechanical stability and reduces dehydration-induced damage (Agati & Tattini, 2010; Vogt, 2010).

Accumulation of caffeoyl tyrosine in *Oeosporangium elegans* under desiccation supports a role for phenylpropanoid metabolism in DT through oxidative stress mitigation, photoprotection, and maintenance of cellular integrity. To the best of our knowledge, this metabolite has not been reported previously in association with DT in plants.

#### 2.3.1.5 Pheophorbide a

Detection of pheophorbide a in desiccated *Oeosporangium elegans* indicates activation of chlorophyll catabolism during dehydration. The compound occupies a central position in porphyrin and chlorophyll metabolism, since it forms during the stepwise breakdown of chlorophyll and then serves as the substrate for pheophorbide a oxygenase (PAO), the committed enzyme of the PAO/phyllobilin route. Turnover through this step prevents phototoxic chlorophyll derivatives from accumulating and driving ROS formation under stress (Pružinská et al., 2003; Tanaka & Tanaka, 2006; Kräutler, 2008; Schelbert et al., 2009; Hörtensteiner & Kräutler, 2011).

Accumulation of pheophorbide a agrees with the decline in chlorophyll content measured here during desiccation, which places pigment breakdown within the regulated desiccation response rather than uncontrolled degradation. In DT plants, controlled chlorophyll catabolism limits photooxidative damage by clearing phototoxic intermediates while cellular integrity is maintained through dehydration (Pružinská et al., 2003; Schelbert et al., 2009; Hörtensteiner & Kräutler, 2011). The process also recovers carbon- and nitrogen-containing metabolites that can be redirected into stress-responsive pathways, which improves metabolic efficiency under severe water deficit (Hörtensteiner, 2006).

Enrichment of the porphyrin and chlorophyll metabolism pathway, and of its chlorophyll degradation branch in particular, reinforces this reading of regulated catabolism during desiccation. Ordered dismantling of the photosynthetic apparatus likely curbs oxidative damage while freeing metabolites for reallocation, contributing to DT in *O. elegans* and to recovery after rehydration. To our knowledge, pheophorbide *a* has not been reported in association with DT, which makes its detection here a novel observation.

#### 2.3.1.6 Epicatechin

The flavonoid biosynthesis pathway represents a critical component of the plant stress response under desiccation conditions. The detection of epicatechin, a terminal flavan-3-ol metabolite. Provides strong evidence for the activation of phenylpropanoid-derived antioxidant mechanisms. Desiccation stress leads to excessive generation of ROS due to disruption of cellular homeostasis and impaired photosynthetic activity. Plants enhance flavonoid biosynthesis to counteract oxidative damage under stress ( Winkel-Shirley, 2001; Falcone Ferreyra et al., 2012).

Epicatechin acts as a potent antioxidant that scavenges ROS and protects cellular macromolecules, including lipids, proteins, and nucleic acids, from oxidative damage. Its hydroxyl-rich structure supports efficient radical neutralization and blocks lipid peroxidation. The compound also contributes to photoprotection, since it absorbs excess radiation, dissipates surplus excitation energy, and reduces photooxidative stress under high light (Brunetti et al., 2013). Accumulation during desiccation agrees with a coordinated response within the wider flavonoid network that supports redox homeostasis and helps preserve cellular integrity (Rice-Evans et al., 1997; Agati et al., 2012; Nakabayashi et al., 2014).

#### 2.3.1.7 3-Hydroxypentadecanoic acid

The detection of 3-hydroxypentadecanoic acid in desiccated *Oeosporangium elegans* suggests that lipid metabolism undergoes substantial reorganization during dehydration. This long-chain hydroxy fatty acid is generally regarded as a structural or metabolic lipid rather than a plant-specific signalling molecule, and its occurrence is consistent with enhanced membrane lipid turnover under stress conditions (Kutschera et al., 2019). Hydroxy fatty acids have been associated with membrane remodelling and oxidative lipid metabolism, indicating that their accumulation may reflect biochemical adjustments required to maintain membrane function during severe water deficit.

Although the specific role of 3-hydroxypentadecanoic acid in plant DT has not been established, its identification in the desiccated metabolome supports the broader involvement of lipid remodeling in the adaptive response of *O. elegans*. To our knowledge, this metabolite has not previously been reported in studies of DT, making its occurrence a potentially novel observation.

The metabolites span diverse biochemical classes, but their concurrent accumulation points to a coordinated response to desiccation rather than a set of independent changes. Arachidoyl ethanolamide and 3-hydroxypentadecanoic acid are lipid-derived and map to membrane lipid remodelling. Epicatechin, caffeoyl tyrosine, and the furochromone derivatives belong to the phenolic and secondary metabolites linked to antioxidant defence. Yuccagenin adds a membrane-associated protective function, and detection of pheophorbide a indicates regulated chlorophyll degradation during dehydration. Each class acts through a distinct mechanism, yet the group as a whole covers membrane remodelling, oxidative stress protection, and photosynthetic adjustment. DT in *Oeosporangium elegans* therefore depends on coordinated metabolic reprogramming across several pathways rather than a single protective mechanism.

Several metabolites were detected in the desiccated state of *Oeosporangium elegans* in the present study. Among these, pheophorbide a proved the most reliable biomarker of desiccation. The compound is a well-characterized intermediate in the chlorophyll degradation pathway within porphyrin and chlorophyll metabolism, and it accumulates when pigment breakdown is active. Its accumulation provides direct evidence for activation of chlorophyll catabolism, a process closely associated with the shutdown of photosynthetic activity under desiccation (Hörtensteiner, 2006).

Our *in vitro* experiments show a substantial reduction in total chlorophyll content (Chl a + b) in *O. elegans* during desiccation (Rudresh et al., 2023). It declined from 1.84 mg $g^{-1}$ FW in hydrated fronds to 0.537 mg $g^{-1}$ FW in desiccated fronds. Literature strongly supports the decrease in total chlorophyll activity during desiccation of plants under going both homoiochlorophyllous desiccation tolerant (HDT) poikilochlorophyllous desiccation tolerant (PDT). We have observed the same in *O. elegans*, where there is a 70.8 % drop in total chlorophyll. Results from this study also show that pheophorbide a, is a central intermediate of the chlorophyll degradation pathway was found to be enriched during desiccation. Chlorophyll degradation therefore stands as an integral part of the desiccation response in *Oeosporangium elegans*. Its signature metabolite, pheophorbide a, accumulates specifically under dehydration and marks a defining feature of the desiccation-induced metabolic profile, one that reflects coordinated physiological adaptation and metabolic reprogramming. Metabolites resolved here give future work a starting point for dissecting the metabolic basis of DT and testing its relevance to drought resilience in crops.

Membrane remodelling emerges as a clear priority for cellular protection. The lipid-derived arachidoyl ethanolamide and hydroxy fatty acids point directly to this process and identify candidate targets for stabilizing membranes under desiccation. Phenolic compounds such as caffeoyl derivatives and flavonoids reinforce antioxidant defence and stress resilience. Considered together, these metabolites open practical routes for metabolite-assisted selection, physiological screening, and metabolic engineering aimed at crop varieties with stronger drought tolerance and improved performance under water-limited conditions.

Although this study provides comprehensive insights into the metabolic reprogramming associated with DT in *Oeosporangium elegans*, the proposed functions of key metabolites are based on metabolite profiling and literature evidence rather than direct experimental validation. The proposed role of pheophorbide *a* as a biomarker requires validation in additional DT and desiccation-sensitive species. In addition, pathway assignments rely on the *Arabidopsis* KEGG database because of the lack of species-specific genomic resources. Future studies

integrating functional validation with transcriptomic and proteomic analyses will further elucidate the molecular mechanisms underlying DT.

## 3. Conclusion:

This study shows that DT in *Oeosporangium elegans* involves a metabolic transition from growth-related processes in the hydrated state to protective and stress-responsive mechanisms under desiccation. Hydrated tissues showed enrichment of primary metabolic pathways along with constitutive secondary metabolism, which agrees with active cellular growth and maintenance. Under desiccation, metabolic reprogramming was extensive and included enhanced lipid metabolism, antioxidant-associated pathways, and regulated chlorophyll catabolism. Chlorophyll content declined and pheophorbide a accumulated, and these two observations provide evidence for controlled chlorophyll degradation during dehydration. Pheophorbide a therefore serves as a candidate biomarker of DT. The concurrent accumulation of lipid-derived and phenolic metabolites further indicates coordinated mechanisms involved in membrane maintenance, oxidative stress protection, and cellular stabilization. Collectively, these findings demonstrate that desiccation tolerance in *O. elegans* is supported by integrated metabolic reprogramming that preserves cellular function during severe water loss and facilitates rapid recovery following rehydration.

## 4. Materials and Method:

### 4.1 Plant Collection and Sample Preparation:

*Oeosporangium elegans* was collected from inselberg crevices at higher elevations, where plants were directly exposed to intense sunlight and low ambient humidity. Sampling was carried out in the Devarayanadurga region of Tumkur district, Karnataka, India (13.378793° N, 77.202446° E), an area characterized by an annual temperature range of 18–25°C and rainfall of approximately 900–1800 mm. Collected samples were immediately placed in sealed plastic containers and transported to the laboratory for further processing.

The collection of plant material were conducted in accordance with the applicable institutional, national, and international guidelines and legislation. The study was performed in accordance with the IUCN Policy Statement on Research Involving Species at Risk of Extinction and the Convention on International Trade in Endangered Species of Wild Fauna and Flora (CITES), where applicable. No specific collection permit or license was required for the collection of plant material from the study site under the applicable regulations. Plant material was collected only in the minimum quantity required for scientific research. The species was identified by Rudresh H. S. and Dr. R. G. Sharathchandra, Department of Studies and Research in Microbiology and Biotechnology, Tumkur University, by comparison with authenticated Herbarium JCB specimens, including Collection No. CS 17023, and standard taxonomic literature (Sankara et al., 2019).

Plants were initially hydrated by allowing them to absorb water until no further increase in fresh weight was recorded, and this fully saturated condition was designated as the hydrated (H) state. Hydrated samples were then subjected to atmospheric air drying, permitting gradual water loss until a constant dry weight was attained, confirming the absence of further moisture loss. This condition was defined as the desiccated (D) state (Rudresh et al., 2023).

### 4.2 Ultra Sonication Assisted Extraction of Metabolites:

0.5 grams fronds of plant (H and D separately - three biological repeats) were weighed and subjected to solvent-based extraction using ethyl acetate and methanol. The samples were homogenized and mixed with 10 mL of ethyl acetate and 10 mL of methanol separately. Homogenized samples were placed in an ultrasonic bath at a frequency of 35 kHz, at room temperature for 30 minutes to facilitate efficient metabolite extraction. After sonication, the extracts were centrifuged at 10,000 rpm for 10 minutes to separate the supernatant. The collected supernatant was then filtered through Whatman filter paper. The extraction procedure was repeated once using fresh solvent to ensure maximum recovery of metabolites. The pooled extracts were concentrated under reduced pressure at temperatures below 40 °C to prevent thermal degradation of metabolites. Finally, the dried extracts were stored at -20 °C until further analysis (Shen et al., 2023).

**4.3 LC–MS/MS Analysis:**

Chromatographic separation was performed using a reverse-phase C18 column (Kinetex®, 250 × 4.6 mm, 5 µm; Phenomenex). The mobile phase consisted of solvent A (water with 0.1% formic acid) and solvent B (methanol with 0.1% formic acid). A gradient elution program was applied at a constant flow rate of 0.5 mL/min. The gradient was initiated with low organic solvent composition and gradually increased to 95% solvent B, followed by re-equilibration to initial conditions. The total run time was 35 min. The injection volume was maintained at 15 µL. Mass spectrometric detection was carried out using a high-resolution Orbitrap mass spectrometer (Thermo Scientific). Data were acquired in full scan mode with subsequent data-dependent MS/MS fragmentation to enable metabolite identification.

**4.4 LC–MS/MS Data Processing:**

The LC–MS/MS datasets obtained from all samples were subjected to an initial quality filtering step to ensure analytical reliability. Only features with a mass error within ±5 ppm was retained to ensure high-confidence annotation and reduce the likelihood of false identifications. Peak area values were used as an estimate of relative metabolite abundance (Zhou et al., 2012).

Metabolites consistently detected across replicates were pooled within each experimental group to minimize variability, and the resulting dataset was analyzed to identify stage-specific patterns of metabolite distribution. Based on occurrence, metabolites were classified into three categories: those unique to the hydrated condition, those specific to the desiccated condition, and those common to both states. This classification integrated qualitative presence–absence information with quantitative abundance data, with presence–absence patterns across replicates evaluated first to establish consistency.

Metabolites associated with the desiccation response were analyzed using the RDKit platform (*Open-source cheminformatics software*. http://www.rdkit.org), which enabled efficient structural processing and organization of the detected compounds. Following LC–MS/MS data acquisition, metabolites were sorted based on their relative abundance and consistent occurrence across biological replicates (Landrum, G., 2016).

**4.5 Metabolite Profiling and Principal Component Analysis:**

Peak area data from three biological replicates of the hydrated and desiccated stages were used for multivariate analysis. For the combine analysis, each metabolite was represented in a six-dimensional feature space comprising its three hydrated- and three desiccated-stage replicate intensities, with a zero value assigned where a metabolite

was not detected in a given stage. Peak areas were log2(x + 1)-transformed and standardised prior to principal component analysis, with the full metabolite set retained throughout. Each stage was additionally analysed separately using its own set of replicate measurements. All analyses were performed in Python 3 (scikit-learn, SciPy, pandas, NumPy)(Van Rossum and Drake, 2009; McKinney, 2010; Harris et al., 2020; Pedregosa et al., 2011; Virtanen et al., 2020; Hunter, 2007), with figures generated in matplotlib at 300 dpi; the full workflow was executed in Google Colab to ensure browser-based reproducibility, and the corresponding code is provided as Supplementary File S1.

**4.6 Metabolite pathway analysis:**

Metabolite pathway analysis was performed using the web-based platform MetaboAnalyst (version 5.0). Identified metabolites obtained from LC–MS/MS analysis for both hydrated and desiccated samples were compiled and subjected to pathway enrichment analysis. The metabolites list was uploaded in compound name format, and pathway analysis was conducted using the *Arabidopsis thaliana* pathway library from the KEGG database as a reference. Over-representation analysis was applied to identify significantly enriched metabolic pathway (Pang et al., 2021).

## 5. References:


1. Agati, G., Brunetti, C., Di Ferdinando, M., Ferrini, F., Pollastri, S., & Tattini, M. (2013). Functional roles of flavonoids in photoprotection: New evidence, lessons from the past. *Plant Physiology and Biochemistry, Plant Phenolics: Biosynthesis, Genetics, and Ecophysiology*, *72*, 35–45. https://doi.org/10.1016/j.plaphy.2013.03.014

2. Agati, G., & Tattini, M. (2010). Multiple functional roles of flavonoids in photoprotection. *New Phytologist*, *186*(4), 786–793. https://doi.org/10.1111/j.1469-8137.2010.03269.x

3. Alejo-Jacuinde, G., & Herrera-Estrella, L. (2022). Exploring the High Variability of Vegetative Desiccation Tolerance in Pteridophytes. *Plants*, *11*(9), Article 9. https://doi.org/10.3390/plants11091222

4. Bentley, J., Moore, J. P., & Farrant, J. M. (2019). Metabolomic Profiling of the Desiccation-Tolerant Medicinal Shrub Myrothamnus flabellifolia Indicates Phenolic Variability Across Its Natural Habitat: Implications for Tea and Cosmetics Production. *Molecules*, *24*(7), 1240. https://doi.org/10.3390/molecules24071240

5. Berglund, T., & Ohlsson, A. B. (2025). The nicotinamide hypothesis revisited—Plant defense signaling integrating PARP, nicotinamide, nicotinic acid, epigenetics, and glutathione. *Febs Letters*, *599*(22), 3355–3368. https://doi.org/10.1002/1873-3468.70146

6. Blancaflor, E. B., Kilaru, A., Keereetaweep, J., Khan, B. R., Faure, L., & Chapman, K. D. (2014). N-Acylethanolamines: Lipid metabolites with functions in plant growth and development. The Plant Journal, 79(4), 568–583. https://doi.org/10.1111/tpj.12427

7. Brunetti, C., Ferdinando, M. D., Fini, A., Pollastri, S., & Tattini, M. (2013). Flavonoids as Antioxidants and Developmental Regulators: Relative Significance in Plants and Humans. *International Journal of Molecular Sciences*, *14*(2), 3540–3555. https://doi.org/10.3390/ijms14023540

8. Challabathula, D., & Bartels, D. (2013). Desiccation tolerance in resurrection plants: New insights from transcriptome, proteome and metabolome analysis. *Frontiers in Plant Science*, *4*. https://www.frontiersin.org/articles/10.3389/fpls.2013.00482

9. Chapman, K. D. (2004). Occurrence, metabolism, and prospective functions of *N*-acylethanolamines in plants. *Progress in Lipid Research*, *43*(4), 302–327. https://doi.org/10.1016/j.plipres.2004.03.002

10. Chapman, K. D., Tripathy, S., Venables, B., & Desouza, A. D. (1998). N-Acylethanolamines: Formation and Molecular Composition of a New Class of Plant Lipids. *Plant Physiology*, *116*(3), 1163–1168. https://doi.org/10.1104/pp.116.3.1163

11. Crider, K. S., Yang, T. P., Berry, R. J., & Bailey, L. B. (2012). Folate and DNA Methylation: A Review of Molecular Mechanisms and the Evidence for Folate's Role2. *Advances in Nutrition*, *3*(1), 21–38. https://doi.org/10.3945/an.111.000992

12. Dace, H. J. W., Reus, R., Ricco, C. R., Hall, R., Farrant, J. M., & Hilhorst, H. W. M. (2023). A horizontal view of primary metabolomes in vegetative DT. *Physiologia Plantarum*, *175*(6), e14109. https://doi.org/10.1111/ppl.14109

13. Dace, H. JW., Adetunji, A. E., Moore, J. P., Farrant, J. M., & Hilhorst, H. WM. (2023). A review of the role of metabolites in vegetative desiccation tolerance of angiosperms. *Current Opinion in Plant Biology*, *75*, 102410. https://doi.org/10.1016/j.pbi.2023.102410

14. Falcone Ferreyra, M. L., Rius, S., & Casati, P. (2012). Flavonoids: Biosynthesis, biological functions, and biotechnological applications. *Frontiers in Plant Science*, *3*. https://doi.org/10.3389/fpls.2012.00222

15. Farnese, F. S., Menezes-Silva, P. E., Gusman, G. S., & Oliveira, J. A. (2016). When Bad Guys Become Good Ones: The Key Role of Reactive Oxygen Species and Nitric Oxide in the Plant Responses to Abiotic Stress. *Frontiers in Plant Science*, *7*, 471. https://doi.org/10.3389/fpls.2016.00471

16. Farrant, J. (2000). A comparison of mechanisms of desiccation tolerance among three angiosperm resurrection plant species. *Plant Ecology*, *151*, 29–39. https://doi.org/10.1023/A:1026534305831

17. Farrant, J. M., Cooper, K., Hilgart, A., Abdalla, K. O., Bentley, J., Thomson, J. A., Dace, H. J. W., Peton, N., Mundree, S. G., & Rafudeen, M. S. (2015). A molecular physiological review of vegetative desiccation tolerance in the resurrection plant Xerophyta viscosa (Baker). *Planta*, *242*(2), 407–426. https://doi.org/10.1007/s00425-015-2320-6

18. Harman-Ware, A. E., Sparks, S., Addison, B., & Kalluri, U. C. (2021). Importance of suberin biopolymer in plant function, contributions to soil organic carbon and in the production of bio-derived energy and materials. *Biotechnology for Biofuels*, *14*, 75. https://doi.org/10.1186/s13068-021-01892-3

19. Harris, C. R., Millman, K. J., van der Walt, S. J., et al. (2020). Array programming with NumPy. *Nature*, *585*, 357–362. https://doi.org/10.1038/s41586-020-2649-2

20. He, M., & Ding, N.-Z. (2020). Plant Unsaturated Fatty Acids: Multiple Roles in Stress Response. *Frontiers in Plant Science*, *11*. https://doi.org/10.3389/fpls.2020.562785

21. Heidarzadeh, A. (2025). RETRACTED ARTICLE: Role of amino acids in plant growth, development, and stress responses: a comprehensive review. *Discover Plants*, *2*(1), 237. https://doi.org/10.1007/s44372-025-00322-0

22. Hörtensteiner, S. (2006a). CHLOROPHYLL DEGRADATION DURING SENESCENCE*. *Annual Review of Plant Biology*, *57*(Volume 57, 2006), 55–77. https://doi.org/10.1146/annurev.arplant.57.032905.105212

23. Hörtensteiner, S. (2006b). CHLOROPHYLL DEGRADATION DURING SENESCENCE*. *Annual Review of Plant Biology*, *57*(Volume 57, 2006), 55–77. https://doi.org/10.1146/annurev.arplant.57.032905.105212

24. Hörtensteiner, S., & Kräutler, B. (2011). Chlorophyll breakdown in higher plants. Biochimica et Biophysica Acta (BBA) - Bioenergetics, Regulation of Electron Transport in Chloroplasts, 1807(8), 977–988. https://doi.org/10.1016/j.bbabio.2010.12.007

25. Hunter, J. D. (2007). Matplotlib: A 2D graphics environment. *Computing in Science & Engineering*, *9*(3), 90–95. https://doi.org/10.1109/MCSE.2007.55

26. Isah, T. (2019). Stress and defense responses in plant secondary metabolites production. *Biological Research*, *52*, 39. https://doi.org/10.1186/s40659-019-0246-3

27. Ivakov, A., Flis, A., Apelt, F., Fünfgeld, M., Scherer, U., Stitt, M., Kragler, F., Vissenberg, K., Persson, S., & Suslov, D. (2017). Cellulose Synthesis and Cell Expansion Are Regulated by Different Mechanisms in Growing Arabidopsis Hypocotyls[OPEN]. *The Plant Cell*, *29*(6), 1305–1315. https://doi.org/10.1105/tpc.16.00782

28. Krasensky, J., & Jonak, C. (2012). Drought, salt, and temperature stress-induced metabolic rearrangements and regulatory networks. *Journal of Experimental Botany*, *63*(4), 1593–1608. https://doi.org/10.1093/jxb/err460

29. Kräutler, B. (2008). Chlorophyll breakdown and chlorophyll catabolites in leaves and fruit. *Photochemical & Photobiological Sciences : Official Journal of the European Photochemistry Association and the European Society for Photobiology*, *7*(10), 1114–1120. https://doi.org/10.1039/b802356p

30. Kutschera, A., et al. (2019). Bacterial medium-chain 3-hydroxy fatty acid metabolites trigger immunity in Arabidopsis. *Science*, 364, 178–181.

31. Lamport, D. T. A., Kieliszewski, M. J., Chen, Y., & Cannon, M. C. (2011). Role of the Extensin Superfamily in Primary Cell Wall Architecture1. *Plant Physiology*, *156*(1), 11–19. https://doi.org/10.1104/pp.110.169011

32. Landrum, G. (2016). RDKit: Open-Source Cheminformatics Software. Available at: RDKit Official Website

33. Li, X.-S., Gao, B., Wood, A., Buitink, J., Zhang, D., & Oliver, M. (2023). Editorial: Desiccation tolerance in land plants: from mechanisms to evolution. *Frontiers in Plant Science*, *14*. https://doi.org/10.3389/fpls.2023.1210946

34. Liu, S., Zenda, T., Tian, Z., & Huang, Z. (2023). Metabolic pathways engineering for drought or/and heat tolerance in cereals. *Frontiers in Plant Science*, *14*. https://doi.org/10.3389/fpls.2023.1111875

35. McKinney, W. (2010). Data structures for statistical computing in Python. In *Proceedings of the 9th Python in Science Conference* (pp. 56–61).

36. Michalak, A. (n.d.). *Phenolic Compounds and Their Antioxidant Activity in Plants Growing under Heavy Metal Stress*.

37. Moffatt, B. A., & Ashihara, H. (2002). Purine and Pyrimidine Nucleotide Synthesis and Metabolism. *The Arabidopsis Book / American Society of Plant Biologists*, *1*, e0018. https://doi.org/10.1199/tab.0018

38. Munnik, T., & Meijer, H. J. G. (2001a). Osmotic stress activates distinct lipid and MAPK signalling pathways in plants. *FEBS Letters, Lisbon Special Issue*, *498*(2), 172–178. https://doi.org/10.1016/S0014-5793(01)02492-9

39. Munnik, T., & Meijer, H. J. G. (2001b). Osmotic stress activates distinct lipid and MAPK signalling pathways in plants. *FEBS Letters, Lisbon Special Issue*, *498*(2), 172–178. https://doi.org/10.1016/S0014-5793(01)02492-9

40. Oliver, M. J., Farrant, J. M., Hilhorst, H. W. M., Mundree, S., Williams, B., & Bewley, J. D. (2020). Desiccation Tolerance: Avoiding Cellular Damage During Drying and Rehydration. *Annual Review of Plant Biology*, *71*, 435–460. https://doi.org/10.1146/annurev-arplant-071219-105542

41. Oliveros, J.C. (2015) Venny. An interactive tool for comparing lists with Venn's diagrams. https://bioinfogp.cnb.csic.es/tools/venny/index.html

42. Osbourn, A. (1996). Saponins and plant defence—A soap story. *Trends in Plant Science*, *1*(1), 4–9. https://doi.org/10.1016/S1360-1385(96)80016-1

43. Oubohssaine, M., Hnini, M., & Rabeh, K. (2024). Exploring lipid signaling in plant physiology: From cellular membranes to environmental adaptation. *Journal of Plant Physiology*, *300*, 154295. https://doi.org/10.1016/j.jplph.2024.154295

44. Pang, Z., Chong, J., Zhou, G., de Lima Morais, D. A., Chang, L., Barrette, M., Gauthier, C., Jacques, P.-É., Li, S., & Xia, J. (2021). MetaboAnalyst 5.0: Narrowing the gap between raw spectra and functional insights. *Nucleic Acids Research*, *49*(W1), W388–W396. https://doi.org/10.1093/nar/gkab382

45. Pedregosa, F., Varoquaux, G., Gramfort, A., et al. (2011). Scikit-learn: Machine learning in Python. *Journal of Machine Learning Research*, *12*, 2825–2830.

46. Pollard, M., Beisson, F., Li-Beisson, Y., & Ohlrogge, J. (2008). Building lipid barriers: Biosynthesis of cutin and suberin. *Trends in Plant Science*, *13*, 236–246. https://doi.org/10.1016/j.tplants.2008.03.003.

47. Pružinská, A., Tanner, G., Anders, I., Roca, M., & Hörtensteiner, S. (2003). Chlorophyll breakdown: Pheophorbide a oxygenase is a Rieske-type iron–sulfur protein, encoded by the accelerated cell death 1 gene. Proceedings of the National Academy of Sciences, 100(25), 15259–15264. https://doi.org/10.1073/pnas.2036571100

48. PubChem Compound Summary for CID 3787294, eicosanoyl-EA. Retrieved April 23, 2026 from https://pubchem.ncbi.nlm.nih.gov/compound/eicosanoyl-EA.

49. Ramaroson, M.-L., Koutouan, C., Helesbeux, J.-J., Le Clerc, V., Hamama, L., Geoffriau, E., & Briard, M. (2022). Role of Phenylpropanoids and Flavonoids in Plant Resistance to Pests and Diseases. *Molecules*, *27*(23), 8371. https://doi.org/10.3390/molecules27238371

50. Ravanel, S., Douce, R., & Rébeillé, F. (2011). Metabolism of Folates in Plants. *Advances in Botanical* Research - ADVAN BOTAN RES, 59, 67–106. https://doi.org/10.1016/B978-0-12-385853-5.00004-0

51. Rolland, F., Baena-Gonzalez, E., & Sheen, J. (2006). SUGAR SENSING AND SIGNALING IN PLANTS: Conserved and Novel Mechanisms. Annual Review of Plant Biology, 57(Volume 57, 2006), 675–709. https://doi.org/10.1146/annurev.arplant.57.032905.105441

52. Rudresh, H. S., Divyashree, T., Yathisha, N. S., Dwarakanath, V., Kumar, H. S. S., & Sharathchandra, R. G. (2023). Comparative analysis of desiccation tolerance in Oeosporangium elegans and Mickelopteris cordata. V*egetos*. https://doi.org/10.1007/s42535-023-00664-8

53. Sankara Rao K, Swamy RK, Deepak K, Singh RA, Gopalakrishna Bhat K (2019b). Flora of Peninsular India. http://peninsula.ces.iisc.ac.in/plants.php?name= Oeosporangiumelegans

54. Schelbert, S., Aubry, S., Burla, B., Agne, B., Kessler, F., Krupinska, K., & Hörtensteiner, S. (2009). Pheophytin Pheophorbide Hydrolase (Pheophytinase) Is Involved in Chlorophyll Breakdown during Leaf Senescence in Arabidopsis. The Plant Cell, 21(3), 767–785. https://doi.org/10.1105/tpc.108.064089

55. Schuster, A.-C., Burghardt, M., Alfarhan, A., Bueno, A., Hedrich, R., Leide, J., Thomas, J., & Riederer, M. (2016). Effectiveness of cuticular transpiration barriers in a desert plant at controlling water loss at high temperatures. *AoB PLANTS*, *8*, plw027. https://doi.org/10.1093/aobpla/plw027

56. Seifert, G. J. (2004). Nucleotide sugar interconversions and cell wall biosynthesis: How to bring the inside to the outside. *Current Opinion in Plant Biology*, *7*(3), 277–284. https://doi.org/10.1016/j.pbi.2004.03.004

57. Shajar, F., Nabi, A. U., Manzoor, A., Saleem, S., Mushtaq, N. U., Manzoor, S., & Rehman, R. U. (2025). Membrane-associated mechanisms in plant responses to abiotic stress. *Plant Science*, *360*, 112726. https://doi.org/10.1016/j.plantsci.2025.112726

58. Shen, L., Pang, S., Zhong, M., Sun, Y., Qayum, A., Liu, Y., Rashid, A., Xu, B., Liang, Q., Ma, H., & Ren, X. (2023). A comprehensive review of ultrasonic assisted extraction (UAE) for bioactive components: Principles, advantages, equipment, and combined technologies. *Ultrasonics Sonochemistry*, *101*, 106646. https://doi.org/10.1016/j.ultsonch.2023.106646

59. Singh, P., Singh, A., & Choudhary, K. K. (2023). Revisiting the role of phenylpropanoids in plant defense against UV-B stress. *Plant Stress*, *7*, 100143. https://doi.org/10.1016/j.stress.2023.100143

60. Stasolla, C., Katahira, R., Thorpe, T. A., & Ashihara, H. (2003). Purine and pyrimidine nucleotide metabolism in higher plants. *Journal of Plant Physiology*, *160*(11), 1271–1295. https://doi.org/10.1078/0176-1617-01169

61. Suresh, K., Zeisler-Diehl, V. V., Wojciechowski, T., & Schreiber, L. (2022). Comparing anatomy, chemical composition, and water permeability of suberized organs in five plant species: Wax makes the difference. *Planta*, *256*(3), 60. https://doi.org/10.1007/s00425-022-03975-3

62. Tanaka, A., & Tanaka, R. (2006). Chlorophyll metabolism. *Current Opinion in Plant Biology, Physiology and Metabolism / Edited by Eran Pichersky and Krishna Niyogi*, *9*(3), 248–255. https://doi.org/10.1016/j.pbi.2006.03.011

63. Teaster, N. D., Motes, C. M., Tang, Y., Wiant, W. C., Cotter, M. Q., Wang, Y.-S., Kilaru, A., Venables, B. J., Hasenstein, K. H., Gonzalez, G., Blancaflor, E. B., & Chapman, K. D. (2007). N-Acylethanolamine Metabolism Interacts with Abscisic Acid Signaling in Arabidopsis thaliana Seedlings. *The Plant Cell*, *19*(8), 2454–2469. https://doi.org/10.1105/tpc.106.048702

64. Tsitsekian, D., Mylona, P., Kamargiakis, E., Rigas, S., & Daras, G. (2025). Developmental and Stress-Mediated Transcriptional Shifts in Riboflavin Metabolism Pathway in Arabidopsis. *Genes*, *17*(1). https://doi.org/10.3390/genes17010016

65. Upchurch, R. G. (2008). Fatty acid unsaturation, mobilization, and regulation in the response of plants to stress. *Biotechnology Letters*, *30*(6), 967–977. https://doi.org/10.1007/s10529-008-9639-z

66. Van Rossum, G., & Drake, F. L. (2009). *Python 3 reference manual*. CreateSpace.

67. Virtanen, P., Gommers, R., Oliphant, T. E., et al. (2020). SciPy 1.0: Fundamental algorithms for scientific computing in Python. *Nature Methods*, *17*, 261–272. https://doi.org/10.1038/s41592-019-0686-2

68. Vogt, T. (2010). Phenylpropanoid Biosynthesis. *Molecular Plant*, *3*(1), 2–20. https://doi.org/10.1093/mp/ssp106

69. Wasternack, C., & Hause, B. (2013). Jasmonates: Biosynthesis, perception, signal transduction and action in plant stress response, growth and development. An update to the 2007 review in Annals of Botany. *Annals of Botany*, *111*(6), 1021–1058. https://doi.org/10.1093/aob/mct067

70. Winkel-Shirley, B. (2001). Flavonoid Biosynthesis. A Colorful Model for Genetics, Biochemistry, Cell Biology, and Biotechnology. *Plant Physiology*, *126*(2), 485–493. https://doi.org/10.1104/pp.126.2.485

71. Zhou, B., Xiao, J. F., Tuli, L., & Ressom, H. W. (2012). LC-MS-based metabolomics. *Molecular bioSystems*, *8*(2), 470–481. https://doi.org/10.1039/c1mb05350g

**Authors Contribution:** Author **a** conceived and designed the study, performed the experiments, analyzed the data, prepared the figures, and wrote the original manuscript. Author **b** contributed to data processing, formal data analysis, and manuscript review. Author **c** contributed to critical revision of the manuscript, provided scientific input and support for the LC–MS/MS analysis. Author **d** and **d*** provided support for the LC–MS/MS analysis, assisted with data interpretation, and critically revised the manuscript. Author **a*** supervised the overall study, provided conceptual guidance, managed the project, and critically reviewed and revised the manuscript. All authors read and approved the final manuscript.

**Funding**

This work was supported by the Anusandhan National Research Foundation (ANRF) under the ANRF PAIR Project (Grant No. ANRF/PAIR/2025/000014/PAIR-B).

**Acknowledgment**

The authors gratefully acknowledge the support and encouragement provided by the Anusandhan National Research Foundation (ANRF). The authors also express their sincere gratitude to all individuals and institutions who contributed to this research through their valuable assistance and support.

**Competing Interests**

The authors declare no competing interests.

**Data Availability**

All data generated and analysed during this study are included in this published article and its Supplementary Information files.

## Supplementary Files

This is a list of supplementary files associated with this preprint. Click to download.

- Metaboanalyst.zip
- DATA.zip
- PCAAnalysis.zip